◆ Human Brain Mapping 34:3216–3232 (2013) ◆

Sustained Attention is Associated with Right Superior Longitudinal Fasciculus and Superior Parietal White Matter Microstructure in Children

Brith Klarborg,[1] Kathrine Skak Madsen,[1,2] Martin Vestergaard,[1] Arnold Skimminge,[1] Terry L. Jernigan,[1,2,3] and William F.C. Baaré[1,2]*

[1]*Danish Research Centre for Magnetic Resonance, Copenhagen University Hospital, Hvidovre, Denmark*
[2]*Center for Integrated Molecular Brain Imaging, Copenhagen, Denmark*
[3]*Center for Human Development, University of California, San Diego, California*

Abstract: Sustained attention develops during childhood and has been linked to the right fronto-parietal cortices in functional imaging studies; however, less is known about its relation to white matter (WM) characteristics. Here we investigated whether the microstructure of the WM underlying and connecting the right fronto-parietal cortices was associated with sustained attention performance in a group of 76 typically developing children aged 7–13 years. Sustained attention was assessed using a rapid visual information processing paradigm. The two behavioral measures of interest were the sensitivity index d' and the coefficient of variation in reaction times (RT_{CV}). Diffusion-weighted imaging was performed. Mean fractional anisotropy (FA) was extracted from the WM underlying right dorsolateral prefrontal (DLPFC) and parietal cortex (PC), and the right superior longitudinal fasciculus (SLF), as well as equivalent anatomical regions-of-interest (ROIs) in the left hemisphere and mean global WM FA. When analyzed collectively, right hemisphere ROIs FA was significantly associated with d' independently of age. Follow-up analyses revealed that only FA of right SLF and the superior part of the right PC contributed significantly to this association. RT_{CV} was significantly associated with right superior PC FA, but not with right SLF FA. Observed associations remained significant after controlling for FA of equivalent left hemisphere ROIs or global mean FA. In conclusion, better sustained attention performance was associated with higher FA of WM in regions connecting right frontal and parietal cortices. Further studies are needed to clarify to which extent these associations are driven by maturational processes, stable characteristics and/or experience. *Hum Brain Mapp 34:3216–3232, 2013.*

Key words: brain maturation; sustained attention; cognitive development; diffusion tensor imaging; fractional anisotropy

Brith Klarborg and Kathrine Skak Madsen have contributed equally to this work.

Contract grant sponsors: Danish Medical Research Council; the Lundbeck Foundation; the Savværksejer Jeppe Juhl og hustru Ovita Juhls Mindelegat Foundation.

*Correspondence to: William F.C. Baaré, Danish Research Centre for Magnetic Resonance, Copenhagen University Hospital, Hvidovre, Kettegaard Allé 30, DK-2650 Hvidovre, Denmark.
E-mail: wimb@drcmr.dk

Received for publication 30 September 2011; Revised 18 April 2012; Accepted 10 May 2012
DOI: 10.1002/hbm.22139
Published online 17 July 2012 in Wiley Online Library (wileyonlinelibrary.com).

INTRODUCTION

Sustained attention is the endogenous controlled capacity to actively detect, select, and respond to relevant stimuli over prolonged periods of time. The ability to focus one's attention is an important cognitive function for everyday life, both by itself and as a modulator or even a prerequisite of higher cognitive functions such as learning or memory [Cowan, 1995; Sarter et al., 2001; Sturm et al., 1997]. Measures of sustained attention have been shown to improve rapidly during the early school-age years and only modestly after the age of 12 [Betts et al., 2006; Lin et al., 1999]. Most studies of sustained attention in children and adolescents have been conducted in clinical samples. Poor sustained attention performance has been associated with several neuropsychiatric disorders with a developmental origin, such as attention deficit hyperactivity disorder (ADHD) [Epstein et al., 1998, 2003; Stins et al., 2005] and schizophrenia [Cattapan-Ludewig et al., 2005; Hilti et al., 2010; Kurtz et al., 2001]. Sustained attention has been extensively investigated in functional and structural imaging studies of adults, but studies in typically developing children and adolescents of sustained attention and its developmental trajectory are sparse (see below). However, such studies are pivotal in elucidating the neurobiological underpinnings of the developmental aspects of sustained attention in humans, and ultimately may contribute to optimizing the diagnosis and treatment of attentional problems. The present study aimed to examine how individual differences in sustained attention performance may be reflected in individual differences in microstructural characteristics of white matter (WM).

The majority of studies investigating neural correlates of sustained attention have used positron emission tomography (PET) or functional magnetic resonance imaging (fMRI), while a few recent studies also employed arterial spin labelling [Demeter et al., 2011; Kim et al., 2006; Lim et al., 2010]. A mostly right-lateralized network in the fronto-parietal cortices has consistently been implicated in studies of healthy adults both across different sensory modalities [Cabeza and Nyberg, 2000; Cohen et al., 1988; Coull, 1998; Lim et al., 2010; Paus et al., 1997] and across different behavioral paradigms [Cabeza and Nyberg, 2000; Cohen et al., 1988; Coull et al., 1996; Ogg et al., 2008; Paus et al., 1997]. However, the extent and exact location of the activations within the fronto-parietal regions varies to some degree. In the frontal region activations centre around the middle frontal gyrus/dorsolateral prefrontal cortex (DLPFC) [Demeter et al., 2011; Kim et al., 2006; Lim et al., 2010; Pardo et al., 1991; Paus et al., 1997; Perin et al., 2010; Sturm et al., 1999], but some studies also showed larger activations spreading to either the inferior or the superior frontal gyrus [Coull et al., 1996; Lawrence et al., 2002, 2003; Lim et al., 2010; Ogg et al., 2008]. In the parietal region, significant activations have been observed in the inferior parietal cortex (PC) [Lim et al., 2010; Ogg et al., 2008; Paus et al., 1997; Sturm et al., 1999], the superior PC [Coull et al., 1996], or both inferior and superior PC [Lawrence et al., 2002, 2003; Perin et al., 2010]. Generally, studies found stronger right than left hemisphere activations. However, the amount of left hemisphere activation differed quite substantially between studies. Sturm et al. [1999] compared functional studies on sustained attention and argued that simple paradigms with no selectivity demands and no warning cues revealed more strongly lateralized right hemisphere activation, whereas any added cognitive complexity resulted in bilateral activations [Corbetta et al., 1991; Coull et al., 1996; Ogg et al., 2008]. The right-lateralized nature of the network supporting sustained attention has also been corroborated by human lesion studies, which accentuated the role of an intact right prefrontal cortex in various tasks of sustained attention [Koski and Petrides, 2001; Molenberghs et al., 2009; Shallice et al., 2008; Wilkins et al., 1987].

Studies investigating how sustained attention performance might be related to microstructural characteristics of the WM in superior longitudinal fasciculus (SLF), which is the main fibre tract connecting frontal and parietal cortices, and the WM underlying frontal and parietal cortices are sparse. Brain microstructure can be investigated in vivo using diffusion-weighted imaging (DWI), which is sensitive to the diffusion of water molecules. WM cellular structures, like the axonal membrane and surrounding myelin sheath, hinder diffusion of water in the direction perpendicular relative to parallel to a fibre bundle, thereby causing diffusion anisotropy [Beaulieu, 2009]. Fitting a diffusion tensor to the DWI data of each voxel provides parallel ($\lambda_{\parallel}$) and perpendicular ($\lambda_{\perp}$) diffusivity measures, as well as the commonly used fractional anisotropy (FA) index. FA reflects the degree of diffusion directionality, which can be influenced by microstructural properties, such as axonal density, diameter, organization, and myelination [Gong et al., 2009]. Several studies, investigating children, adolescents, and/or young adults between 5 and 30 years of age, have reported age-related increases in FA in multiple WM locations, reflecting a disproportionate decrease in $\lambda_{\perp}$ relative to $\lambda_{\parallel}$, possible due to ongoing myelination, increased axonal diameter, and/or increased axonal density [Eluvathingal et al., 2007; Lebel et al., 2008; Perrin et al., 2009; Snook et al., 2005]. Diffusion tensor imaging (DTI) has been successfully employed in elucidating associations between WM microstructure of specific anatomical structures and a number of cognitive functions, e.g., visuo-spatial working memory [Klingberg, 2006; Olesen et al., 2003; Vestergaard et al., 2011], visual search [Mabbott et al., 2006], and response inhibition [Madsen et al., 2010].

Several studies have reported on the relationship between WM microstructure and measures that involve sustained attention in clinical populations. Bonnelle et al. [2011] examined traumatic brain injury patients and measured sustained attention as a change in RTs over time on a simple choice RT task. Patients with greater sustained attention deficits (e.g., higher RT change) had lower FA in

the right cingulum. Pfefferbaum et al. [2010] investigated alcoholics using the Digit Symbol Test [Wechsler, 1981], which involves many component processes including executive functions, sustained attention, associative learning, and psychomotor speed. The authors investigated fibre tracts traversing the corpus callosum (CC) and observed associations between Digit Symbol test scores and DWI measures that were mainly restricted to the prefrontal CC region. Dineen et al. [2009] investigated multiple sclerosis patients using the Paced Auditory Addition Test [PASAT; Rao's adaptation of the Gronwall administration; Rao et al., 1991], a test of sustained attention, working memory and processing speed. Using a voxel-wise approach with tract-based spatial statistics [TBSS, Smith et al., 2006], the authors found that after controlling for multiple sclerosis severity PASAT performance was associated with FA in the left side of the body and splenium of the corpus callosum radiating into the left parieto-occipital region, the left cingulum and the parietal arc of the left arcuate fasciculus.

A few studies have reported on associations between WM microstructure and measures that involve sustained attention in healthy subjects. Mabbott et al. [2006] investigated a small group ($N = 17$) of typically developing children and adolescents aged 6–17 years and found that associations between the standard error of reaction times (RTs) on the Connors Continuous Performance Task II [Conners, 2000] and FA within the left internal capsule, posterior body of the corpus callosum, and 11 out of 12 WM compartments did not persist after controlling for age. Takahashi et al. [2010] found that in healthy adult subjects the sensitivity index d' of the Conners Continuous Performance Task—Identical Pairs [Cornblatt et al., 1988] was associated with right cingulum FA, but not with WM within a fronto-parietal network. In another study, the ADHD score of the test of variables of attention [TOVA: Leark et al., 2007] was significantly positively correlated with FA of right SLF in both adult ADHD patients and matched healthy controls [Konrad et al., 2010]. Although there is anatomical consistency between this finding and the many reports of right-sided fronto-parietal activations in functional studies, the ADHD score is a complex score possibly loading on many cognitive processes, which makes it less suitable for finding neural correlates of sustained attention.

In the present study, we investigated the relationship between sustained attention performance and WM microstructure in a large cohort of 76 typically developing children between 7 and 13 years of age. We hypothesized that higher FA in WM underlying the right DLPFC and PC and in the right SLF would be associated, independently of age, with better performance on the rapid visual information processing (RVP) test of sustained attention. The adjustment for age attempts to account for the fact that both FA measures [Lebel et al., 2008, 2011] and performance on tests of sustained attention [Betts et al., 2006; Lin et al., 1999] is known to improve as a function of age in the investigated age range. Simple correlations among these variables without correcting for the effects of age would therefore provide little evidence for any direct relationship between the WM measures and sustained attention performance. Sustained attention performance was measured with the sensitivity index d', which is a measure that expresses the subject's ability to detect signals independent of the subjects' answering strategy or bias. Moreover, we investigated whether the coefficient of variation in RTs (RT_{CV}), a measure of RT variability, was associated with the same areas as d'. Finally, to investigate the anatomical specificity of any observed associations between sustained attention performance measures and FA of the right hemispheric regions-of-interest (ROIs), planned follow-up analyses controlled for FA of the equivalent anatomical ROIs in the left hemisphere or mean global WM FA.

MATERIALS AND METHODS

Subjects

Ninety-two typically developing children (55 female) aged 7–13 (mean = 10.03, standard deviation (SD) = 1.66) years were recruited for a longitudinal study of brain and behavioral development from three schools in the Copenhagen suburban area. Prior to participation and after receiving oral and written explanation of the study aims and study procedures, all children assented to the procedures and informed written consent was obtained from the parents/guardians of all subjects. According to parent questionnaires, no subjects had any known history of neurological or psychiatric disorders, or significant brain injury. The project was approved by the Danish Committee for Biomedical Research Ethics (H-KF-01-131/03), and conducted in accordance with the Declaration of Helsinki.

After evaluating the images for both incidental findings and image quality, images from a total of 16 subjects (9 females) were excluded from further analyses due to poor quality of the DWI data ($n = 12$), incomplete scanning sessions ($n = 3$), or incidental findings ($n = 1$). These 16 subjects did not differ significantly from the remaining 76 subjects on age (Mann–Whitney $U = 464.5$, $P = 0.139$), gender ($\chi^2 = 2.130$, $P = 0.144$), handedness ($\chi^2 = 0.705$, $P = 0.401$), or parent education (Mann–Whitney $U = 472.5$, $P = 0.162$). Demographic data for the included subjects are presented in Table I. The present study includes data from the baseline of the ongoing longitudinal brain maturation research project. The imaging data have also been used in studies on spatial working memory [Vestergaard et al., 2011], visuospatial choice reaction time [Madsen et al., 2011] and response inhibition [Madsen et al., 2010].

Behavioral Test

Sustained attention was measured using the "age 7–14" edition of the RVP paradigm from the CANTAB battery

TABLE I. Demographic data for the included subjects

	1st/2nd graders	3rd/4th graders	5th/6th graders	All subjects
Age (Mean ± SD)	8.20 ± 0.48	10.11 ± 0.37	12.20 ± 0.36	10.14 ± 1.63
Gender (female/male)	14/10	16/13	14/9	44/32
Handedness (right/left)	21/3	24/5	21/2	66/10
Parents' years of education (Mean ± SD)	14.0 ± 1.7	13.4 ± 2.0	13.7 ± 2.0	13.7 ± 1.9

Children from three different school grade levels were included in the study. The children were scanned just before (when in first, third or fifth grade) or just after (when in second, fourth or sixth grade) the summer vacation.

(Cambridge Cognition, Cambridge, UK). Numbers from two to nine were presented as figures one at a time in a pseudo-random order in the centre of a 12-inch computer screen. The numbers appeared in white on a black background inside a white outlined box. Each number was presented for 600 ms and directly followed by the next number in the stream of stimuli (Fig. 1). The task was to detect the target sequence "3-5-7" and respond by pressing a button on a response pad with the dominant hand. The target sequence was written on the screen next to the white box to reduce the memory demand during the test. Responses were categorized as a hit from 100 ms after the third number of the target sequence was presented and during the two numbers following the target sequence (potential RT range: 100–1800 ms). There was a minimum of two numbers between each target sequence to allow equal response time. The targets were presented with a frequency of 4 targets/30 s. The task was preceded by a training period of 2 min with gradually disappearing prompts (targets presented in different color, underlined, and with a beep sound). After the training period, a 4-min test period started. However, the first minute of the test period was regarded as practice, so that all subjects had time to get used to the no-prompt version of the paradigm, and only data from the three remaining minutes were analyzed.

The RVP test produced the four classic outcome variables of signal detection, namely hits, misses (errors of omission), false alarms (errors of commission), and correct rejections. These measures were combined in the calculation of the sensitivity index d' [Swets, 1961] (d' = Z(# hits/(# hits + # misses)) – Z(# false alarms/(# false alarms + # correct rejections))). As d' cannot be calculated when hit and false alarms rates are 1 or 0, scores were corrected by one quarter observation (e.g., hits = 23.75, false alarms = 0.25) in case of a maximal number of hits (=24) or zero false alarms. One subject had 24 hits, seven subjects had zero false alarms, and four subjects had both 24 hits, and zero false alarms. A high d' indicates good signal detection. The advantage of d' is that it gives a complete expression of the sensitivity to targets, as opposed to using hits uncorrected for the number of false alarms [Lawrence et al., 2003]. At the same time d' is a relatively simple score compared to some of the measures provided by more clinically oriented tests [Konrad et al., 2010; Leark et al., 2007]. Besides d', the RT_{CV} was calculated, which is the SD of the RT for hits divided by the mean RT for hits. This measure was used, because it controls for the situation where longer RTs vary more than shorter ones simply because they are farther away from the floor [Stuss et al., 2003]. A lower RT_{CV} indicates that the subject is responding with similar RTs throughout the test (good performance), whereas a higher RT_{CV} could be caused by lapses of attention or a time-on-task effect.

Image Acquisition

All scans were acquired on the same day as the RVP-test session using a 3T Siemens Magnetom Trio MR

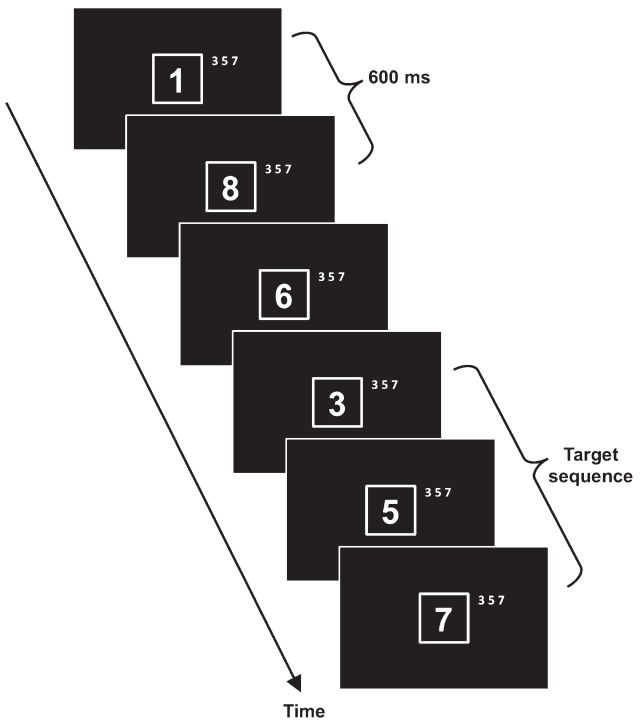

Figure 1.

Graphical representation of the rapid visual information processing (RVP) paradigm. A continuous stream of one digit numbers was presented centrally on the computer screen. Each number was presented for 600 ms (no gaps). The task was to detect the target sequence "3-5-7."

scanner (Siemens, Erlangen, Germany) with an eight-channel head coil (Invivo, FL). Whole brain DWI were acquired using a twice-refocused balanced spin echo sequence that minimized eddy current distortion [Reese et al., 2003] with 10 non-diffusion-weighted images ($b = 0$) and 61 diffusion-weighted images ($b = 1{,}200$ s mm^{-2}) encoded along independent collinear diffusion gradient orientations [Jansons and Alexander, 2003] (TR = 8,200 ms; TE = 100 ms; FOV = 220 × 220; matrix = 96 × 96; GRAPPA: factor = 2; lines = 48; number of axial slices (no gap) = 61; voxel size = 2.3 × 2.3 × 2.3 mm^3, acquisition time = 9.50). An axial gradient echo-based field map sequence was acquired to correct for geometric distortions due to B_0 magnetic field inhomogeneities (TR = 530 ms; TE = 5.19/7.65 ms; FOV = 256 × 256; matrix = 128 × 128; number of slices (no gap) = 47; voxel size = 2 × 2 × 3 mm^3, acquisition time = 2.18). A sagittal whole brain 3D turbo spin echo sequence was used to acquire T2-weighted images for generating a brain mask (TR = 3,000 ms; TE = 354 ms; FOV = 282 × 282; matrix = 256 × 256; number of slices = 192; voxel size = 1.1 × 1.1 × 1.1 mm^3, acquisition time = 8.29). All the scan acquisitions were aligned parallel to the anterior commissure-posterior commissure line.

Image Preprocessing

Prior to image processing, the image quality of all imaging data was visually inspected (blind to behavioral data) to ensure the quality of the data, and an experienced neuroradiologist evaluated all subjects' images with regards to incidental findings. Preprocessing of images was done with pipelines implemented in Matlab, using mainly SPM5 routines. Diffusion-weighted images were oriented to the MNI coordinate system. This was done by coregistering the mean b0 image to the T2-weighted image using a six-parameter mutual information rigid transformation. Subsequently, all diffusion-weighted images (no reslicing) were coregistered to the mean b0 image. Geometric distortions in the coregistered images were corrected using a voxel displacement map based on both the acquired B_0 field map [Andersson et al., 2001] and a scanner specific map of gradient non-linearities [Jovicich et al., 2006]. Next, all images were resliced using trilinear interpolation with a single reslicing step. The diffusion gradient orientations were adjusted to account for any rotation during the registration. The diffusion tensor was fitted using the RESTORE algorithm with a noise standard deviation of 30 [Chang et al., 2005], implemented in Camino [Cook et al., 2006]. Hereafter FA, and diffusivities parallel ($\lambda_{\|} = \lambda_1$) and perpendicular ($\lambda_{\perp} = (\lambda_2 + \lambda_3) / 2$) to the principal diffusion direction were calculated. A brain mask based on T2-weighted images was applied on FA and diffusivity images. The mask was created using segmentation routines and morphological operations implemented in the VBM5 toolbox (http://dbm.neuro.uni-jena.de/vbm/vbm5-for spm5/) in SPM5.

Intersubject Spatial Normalization of Fibre Tracts

Fibre tracts were spatially normalized and aligned across subjects to permit delineation of specific ROIs (see below) in a common anatomical framework. This was achieved by employing the TBSS module in FSL 4.1.0 [Smith et al., 2006]. The FA images of all subjects were aligned into a common space using the non-linear registration tool FNIRT [Andersson et al., 2001]. Next, the most representative FA image was identified by non-linearly registering the FA images of all subjects to the FA images of every other subject, and then used as a study-specific target. The target was aligned to MNI space using affine registration, and subsequently the entire dataset was aligned and transformed into 1 mm^3 MNI space. A mean FA image was created across subjects, and thinned to create a mean FA skeleton, representing the centres of tracts common to all subjects. The skeleton was subsequently thresholded at FA > 0.25. The skeleton contained 103,588 1 mm^3 interpolated voxels, equivalent to approximately one fourth of the voxels above threshold. Each subject's aligned FA image was then projected onto the skeleton by locating the voxels with the highest local FA value in the direction perpendicular to the skeleton tracts and assigning this value to the skeleton at this standardized location. This results in a mapping of each voxel location in the skeleton to a specific voxel in the individual FA maps. The nonlinear warps and skeleton projections were also applied to $\lambda_{\|}$ and $\lambda_{\perp}$ data. Finally a color-coded target FA map was generated by applying the affine transformation created when the target FA image was aligned to MNI space, to the target's primary eigenvector (v_1) image using the "vecreg" command in FSL.

Regions-of-Interest

To test our primary hypothesis, we delineated three ROIs, namely, the right SLF, and the WM underlying the right DLPFC and the right PC (Fig. 2). ROIs in the equivalent anatomical areas in the left hemisphere were delineated for use in analyses of anatomical specificity. ROIs were drawn in FSLview 4.1.0 onto the mean FA skeleton overlaid on the color-coded study-specific target FA map. Notice that the SLF ROIs are equivalent to the ones applied in the study by Vestergaard et al. [2011]. The DLPFC and parietal ROIs were based on earlier findings in studies of sustained attention [Coull et al., 1996; Lawrence et al., 2003; Ogg et al., 2008; Pardo et al., 1991; Paus et al., 1997] and therefore they were drawn independently as described below and differ slightly from the ROIs used by Vestergaard et al. [2011].

The SLF ROIs were delineated using the atlas of human white matter [Mori et al., 2004] and the color-coded target FA map. The SLF ROIs only included white matter voxels with anterior–posterior oriented eigenvectors (green in the color-coded FA map in Fig. 2b). The anterior and posterior

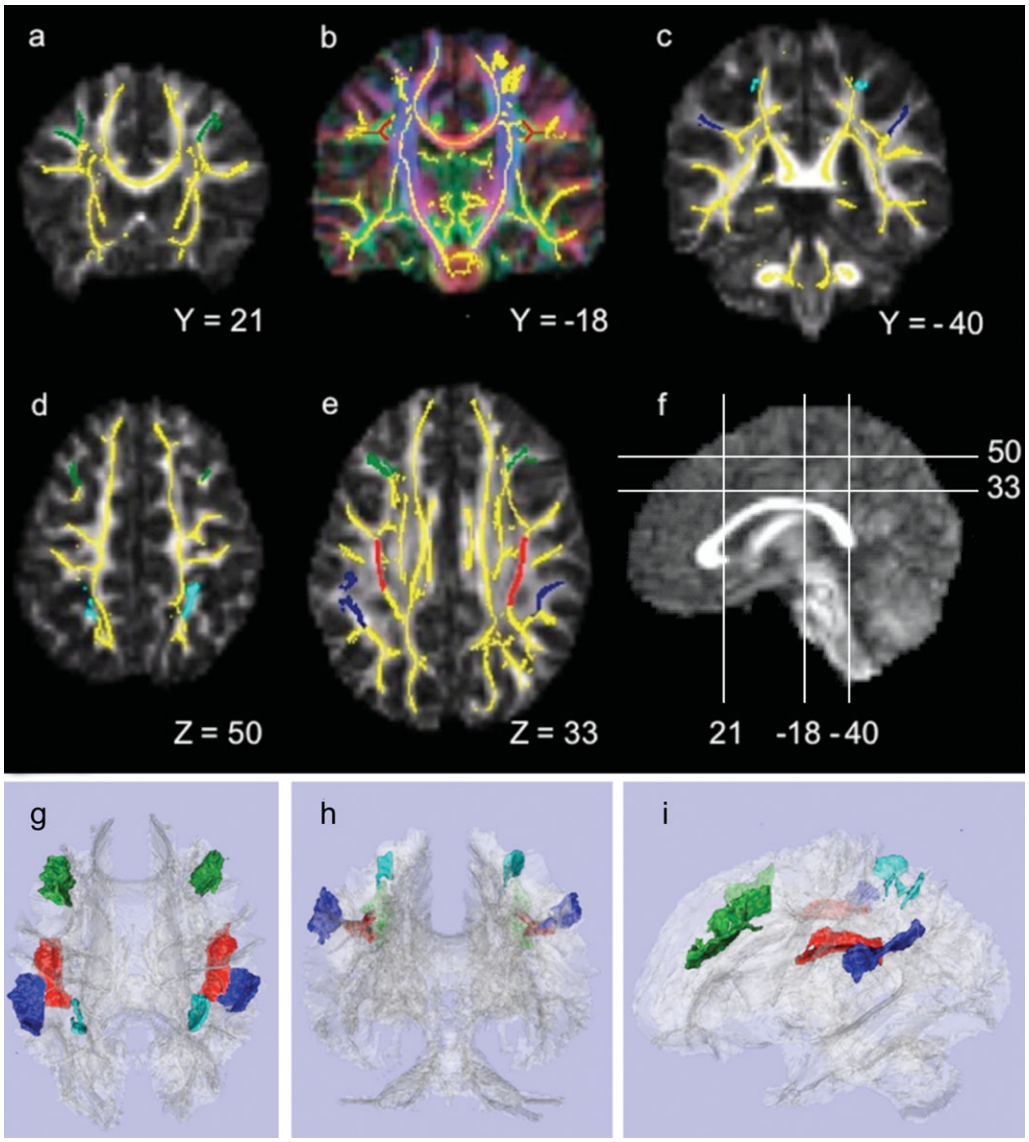

Figure 2.

Regions-of-interest (ROIs) displayed on the mean tract-based spatial statistics (TBSS) skeleton (yellow), overlaid on the target's fractional anisotropy (FA) map, gray scale in **a**, **c**, and **d**, and color-coded based on the direction of the primary eigenvector in **b**, where the primary diffusion direction is colored as: red = left/right, green = anterior/posterior, and inferior/superior. (a) Dorsolateral prefrontal cortex (DLPFC) ROIs in green at coronal slice $Y = 21$; (b) Superior longitudinal fasciculus (SLF) ROIs in red at coronal slice $Y = -18$; (c) Parietal cortex (PC) ROIs in blue, inferior part in dark blue and superior part in light blue, at coronal slice $Y = -40$; (d) DLPFC and superior PC ROIs in green and light blue, respectively, at axial slice $Z = 50$; (**e**) DLPFC, SLF and inferior PC ROIs in green, red and dark blue, respectively, at axial slice $Z = 33$; (**f**) Mid-sagittal slice displaying the mapping of slices a–d. All coordinates refer to MNI space. **g**, **h**, and **i** show 3D renderings of the ROIs and the mean TBSS skeleton (light gray) from respectively superior, posterior, and left viewing angles; DLPFC in green; SLF in red; inferior and superior PC in respectively dark and light blue. Left is left (neurological convention).

boundaries of the SLF ROIs were set according to the DLPFC and PC ROIs used in Vestergaard et al. [2011]. The right and left SLF ROI contained 736 and 745 voxels, respectively.

The borders of the DLPFC and PC ROIs were determined using a human brain atlas [Duvernoy and Bourgouin, 1999]. The DLPFC ROIs consisted of WM underlying the cortex of the middle frontal gyrus, largely

corresponding to Brodmann area 46 and the inferior part of area 9. The anterior boundary of the DLPFC ROIs was set at the coronal slice anterior to the genu of the corpus callosum ($Y = 36$) to exclude white matter skeleton voxels in the frontopolar region. The posterior border was delineated by the precentral sulcus. The superior boundary was delineated by the superior frontal sulcus, and the inferior boundary by the inferior frontal sulcus. The medial border was delineated according to the depth of the superior and inferior frontal sulci on coronal slices by connecting the most inferior-medial point of the superior frontal sulcus to the most inferior-medial point of the inferior frontal sulcus with a straight line (see Fig. 2a). The right DLPFC ROI included 999 voxels, whereas the left included 1,204 voxels.

The parietal ROI included WM underlying the inferior (supramarginal gyrus) and superior PC divided by the intraparietal sulcus, but not the WM connecting the two lobules. Thus, the ROI included two non-touching parts (Fig. 2c). The anterior boundary for both PC ROIs was the postcentral sulcus. For the inferior PC ROIs, the inferior boundary was defined by the Sylvian Fissure (and the terminal ascending segment), the medial boundary by the lateral border of the SLF ROIs, and the posterior border by a horizontal line through the most anterior-medial point of the ascending segment of the superior temporal sulcus on axial slices. The superior PC ROIs, included only skeleton segments underlying area 7PC as defined by the probabilistic Juelich histological atlas included in FSLview [Scheperjans et al., 2008]. The lateral border was defined by the intraparietal sulcus. Skeleton segments underlying the superior parietal PC branching medially towards the precuneus were excluded. The right PC ROI consisted of 811 voxels with 493 voxels in the inferior part and 318 in the superior part. Left PC ROI consisted of 954 voxels with 777 and 177 voxels in the inferior and superior part, respectively. 3D representations of the extracted ROIs are depicted in Figure 2.

Statistical Analysis

The software package SPSS, version 18.0 (SPSS, Chicago, IL) was used for statistical analyses. Behavioral measures and ROI FA values were tested for gender effects using *t* tests, and age effects using linear regression. Multiple linear regression was used to test our hypotheses. Shapiro-Wilk tests showed that all data were normally distributed except for RT_{CV}. A logarithmic transformation of RT_{CV} normalized the residuals. All other assumptions for linear regression were fulfilled. Tests were considered significant when $\alpha \leq 0.05$.

The primary hypothesis was tested using a hierarchical model. First, age was entered as the only predictor variable of the RVP performance measure d'. Second, FA values of the right SLF, DLPFC and PC ROIs were entered simultaneously as additional predictors. If entering the ROIs resulted in a significant R^2 change, the ROIs were considered to be collectively associated with d'. Subsequently, it was determined which ROIs significantly contributed to the association.

Planned follow-up analyses were contingent on observing significant results in the primary analyses. All models described below included age as a covariate. First, contingent on a significant association with right PC, we investigated the relative contributions of the inferior and superior PC. Next, the anatomical specificity of observed associations between individual right ROIs and d' was tested by including either global WM FA (mean TBSS skeleton FA), or FA of the corresponding left hemisphere ROI as a predictor. Finally, for the ROIs exhibiting a significant association with d' we investigated if they were also associated with RT_{CV}, and contingent on an association anatomical specificity was assessed as described above. When a ROI was associated with both behavioral measures, we tested whether the associations between ROI FA and behavioral measures were independent of a correlation between the two behavioral measures. To this end two models were created: one in which RT_{CV} was included as an additional predictor of d', and one in which d' was included as an additional predictor of RT_{CV}.

The $\lambda_{\parallel}$ and $\lambda_{\perp}$ were investigated to further explore the nature of observed FA findings, since higher FA could be due to increased $\lambda_{\parallel}$ and/or decreased $\lambda_{\perp}$. This was tested by replacing the ROI FA variables with either $\lambda_{\parallel}$ or $\lambda_{\perp}$ in the models where the ROI FAs were significant.

Post hoc analyses were conducted in which gender was included in the models described above.

An effect size map is presented to provide further anatomical information about the association between d' and FA values across the WM skeleton [Jernigan et al., 2003]. The effect size map is a *t*-map of the correlation between FA and d', adjusted for age. The t-map was generated in FSL using whole-brain linear regression across the whole skeleton with d' and age as predictors and FA as the dependent variable. Voxel level *t* value range cut-off points for both positive (red-yellow) and negative (blue-light blue) correlations ($df = 74$) were $t = \pm 2.644$ ($P = 0.01$), $t = \pm 1.993$ ($P = 0.05$), $t = \pm 1.293$ ($P = 0.20$). Please note that these *t* values are not corrected for multiple comparisons.

RESULTS

RVP performance measures and ROI FA values are presented in Table II. Scatter plots of RVP and ROI FA measures against age are presented in Figures 3 and 4, respectively. Age was significantly and positively related to d' ($r_{(74)} = .572$, $P < 0.001$) and negatively to RT_{CV} ($r_{(74)} = -0.337$, $P = 0.003$), indicating that with increasing age participants became better in sustaining attention. There was no effect of gender on d' ($r_{(74)} = -0.096$, $P = 0.412$) or RT_{CV} ($r_{(74)} = 0.93$, $P = 0.423$). The correlation between d' and RT_{CV} was $r_{(74)} = -0.47$ ($P < 0.001$). Generally, ROI FA significantly increased with increasing age ($r_{(74)}$ *-range* =

TABLE II. RVP performance and FA measures presented by grade level

		1st/2nd graders	3rd/4th graders	5th/6th graders	All subjects
RVP performance					
d′		2.882 ± 0.713	3.524 ± 0.638	4.113 ± 0.797	3.499 ± 0.856
RT_{CV}[a]		0.388 ± 0.117	0.346 ± 0.113	0.294 ± 0.090	0.344 ± 0.113
FA					
SLF	Right	0.465 ± 0.029	0.471 ± 0.028	0.493 ± 0.030	0.476 ± 0.031
	Left	0.485 ± 0.032	0.489 ± 0.029	0.513 ± 0.029	0.495 ± 0.032
DLPFC	Right	0.420 ± 0.030	0.419 ± 0.034	0.428 ± 0.031	0.422 ± 0.031
	Left	0.397 ± 0.024	0.404 ± 0.027	0.418 ± 0.023	0.405 ± 0.026
PC (total)	Right	0.393 ± 0.033	0.398 ± 0.039	0.413 ± 0.033	0.401 ± 0.036
	Left	0.386 ± 0.024	0.402 ± 0.031	0.406 ± 0.033	0.399 ± 0.031
Only inferior PC	Right	0.399 ± 0.027	0.400 ± 0.045	0.414 ± 0.036	0.404 ± 0.037
	Left	0.387 ± 0.029	0.404 ± 0.033	0.407 ± 0.036	0.400 ± 0.033
Only superior PC	Right	0.385 ± 0.060	0.393 ± 0.048	0.411 ± 0.039	0.396 ± 0.051
	Left	0.382 ± 0.046	0.395 ± 0.045	0.402 ± 0.041	0.393 ± 0.044
Global WM		0.450 ± 0.015	0.459 ± 0.018	0.467 ± 0.013	0.459 ± 0.017

Rapid visual information processing (RVP) performance and fractional anisotropy (FA) measures presented as mean ± standard deviation (SD) for the three different school grade levels included in the study. RVP performance measures include the sensitivity index d′ and the coefficient of variation in reaction times (RT_{CV}); Mean FA values presented for the superior longitudinal fasciculus (SLF), the white matter (WM) underlying dorsolateral prefrontal cortex (DLPFC) and parietal cortex (PC) (total, inferior and superior values), and global WM.

[a]Note that the RT_{CV}'s presented here are the raw data, and not the logarithmic transformation used in the statistical analyses.

0.234–0.397, *P range = 0.042–0.00003*), except for right DLPFC ($r_{(74)}$ = 0.136, *P* = 0.242), right inferior ($r_{(74)}$ = 0.182, *P* = 0.116) and left superior PC ($r_{(74)}$ = 0.144, *P* = 0.216). A significant gender effect (male > female) was observed for left DLPFC FA ($r_{(74)}$ = 0.244, *P* = 0.034), but not for any other ROI ($r_{(74)}$ *-range* =−0.215–−0.009, *P range = 0.062–0.938*).

Associations Between *d′* and the Fronto-Parietal Network

Results of the hierarchical regression used to test our primary hypothesis are presented in Table III. First, age was entered as the only predictor variable of the RVP performance measure *d′* (Table III, Model 1). Next, the FA

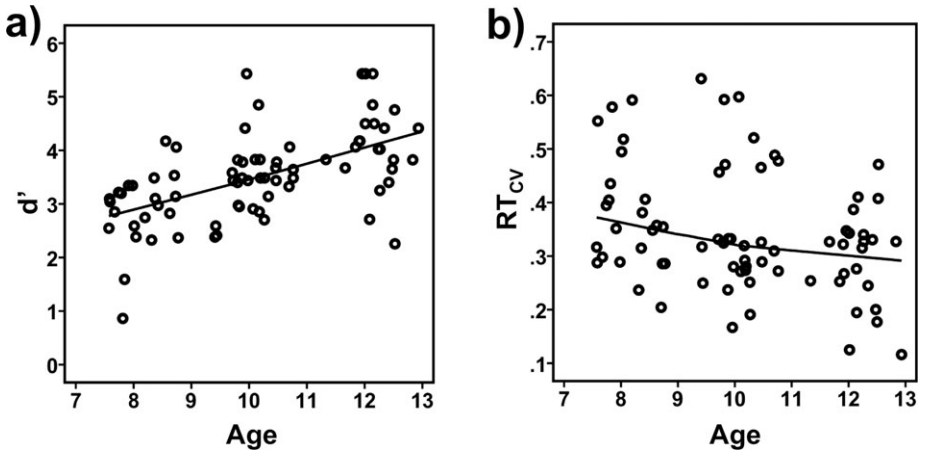

Figure 3.

Scatterplots of (**a**) the sensitivity index *d′*, and (**b**) coefficient of variation in the reaction time (RT_{CV}) by age (in years). Participants were significantly better to sustain attention with increasing age, as reflected in increasingly higher *d′* and lower RT_{CV} scores (see Result section for details). To visualize the relationships across age Loess fit lines using the Epanechnikov kernel to smooth 99% of data points were applied to the data.

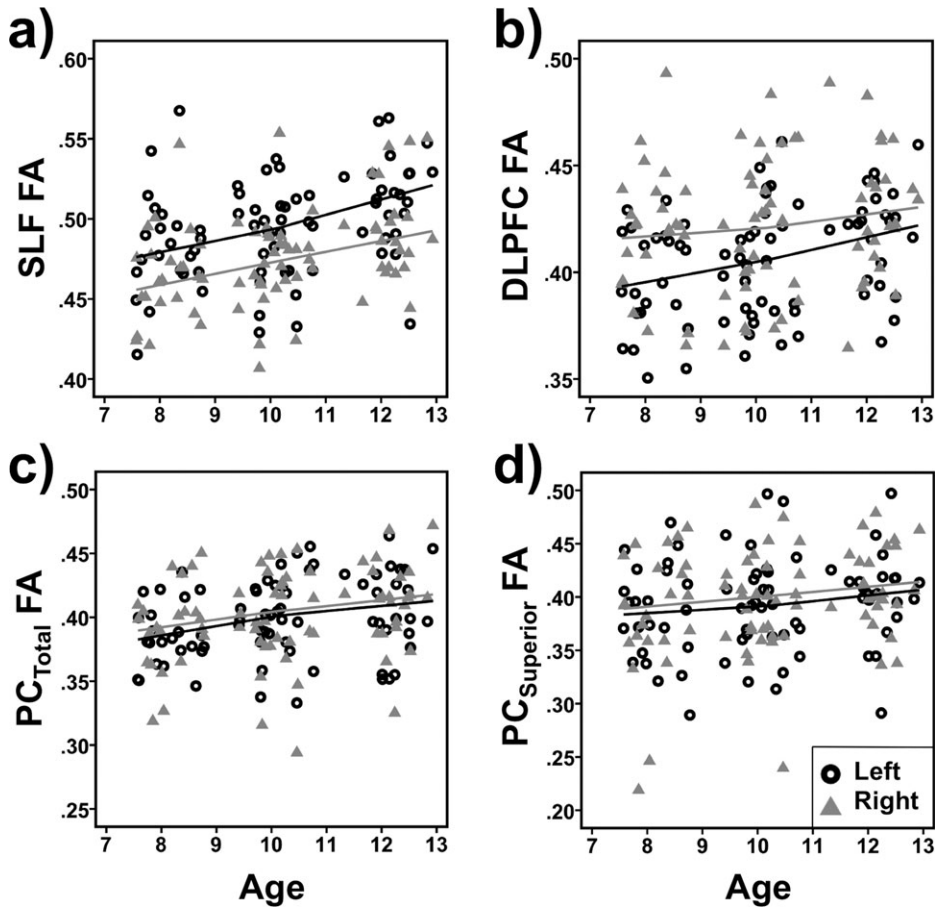

Figure 4.

Scatterplots of fractional anisotropy (FA) of the left and right (**a**) superior longitudinal fasciculus (SLF) and white matter underlying (**b**) dorsolateral prefrontal cortex (DLPFC), (**c**) parietal cortex (PC_{Total}), and (**d**) superior parietal cortex ($PC_{Superior}$) by age (in years). Generally, ROI FA significantly increased with increasing age, except for right DLPFC and left superior PC (see result section for details). To visualize the relationships across age Loess fit lines using the Epanechnikov kernel to smooth 99% of the data points were applied to the data.

values of the right SLF, DLPFC, and PC ROIs were entered simultaneously as additional predictors (Table III, Model 2). In both models age was significantly associated with d'. As hypothesized, there was a significant increase in variance explained by Model 2 relative to Model 1 showing that better sustained attention (i.e., increased d' scores) was significantly associated with higher FA in the right fronto-parietal network (SLF, DLPFC, and PC) independently of age (R^2 change $_{\text{Model 2–Model 1}} = 0.113$, $F_{(1,74)} = 4.792$, $P = 0.0043$). Closer inspection of Model 2 revealed

TABLE III. Fronto-parietal FA relationship to RVP d' (sensitivity index), *a priori* hypothesis

				Age			FA Right SLF			FA right DLPFC			FA right PC		
Model	Dependent variable	R^2	*df*	β	*t*	*p*	β	*t*	*p*	β	*t*	*p*	β	*t*	*p*
1	d'	0.327	74	0.572	5.991	*0.00000007*									
2	d'	0.440[a]	71	0.425	4.358	*0.000044*	0.267	2.571	***0.012***	−0.090	−0.932	***0.35***	0.212	2.179	***0.033***

Hierarchical regression on the rapid visual information processing (RVP) measure d' with age, and fractional anisotropy (FA) of the three regions-of-interest (ROIs), namely right superior longitudinal fasciculus (SLF), and white matter underlying dorsolateral prefrontal cortex (DLPFC) and parietal cortex (PC). Significant associations are printed italic, with those related to FA-measures additionally printed in bold.

[a] R^2 change $_{\text{model 2 - model 1}} = .113$, $F_{(1,74)} = 4.792$, $P = 0.0043$.

TABLE IV. Follow-up analyses testing the specificity of right SLF FA associations with RVP *d′*

				Age			Right SLF FA			Left SLF FA			Global WM FA		
Model	Dependent variable	R^2	*df*	β	*t*	*p*	β	*t*	*p*	β	*t*	*p*	β	*t*	*p*
1	*d′*	0.401	73	0.454	4.597	*0.000018*	0.297	3.007	***0.004***						
2	*d′*	0.403	72	0.468	4.535	*0.000022*	0.328	2.796	***0.007***				−0.060	−0.498	0.62
3	*d′*	0.401	72	0.453	4.540	*0.000022*	0.292	2.037	***0.045***	0.006	0.046	0.964			
4	*d′*	0.366	73	0.495	4.959	*0.00000045*				0.213	2.139	***0.036***			
5	*d′*	0.366	72	0.489	4.738	*0.0000011*				0.222	1.796	0.077	−0.015	−0.113	0.91

Multiple regression on the rapid visual information processing (RVP) measure *d′* with age, and fractional anisotropy (FA) of right and left superior longitudinal fasciculus (SLF), and global white matter (WM). Significant associations are printed italic, with those related to FA-measures additionally printed in bold.

that only FA of the right SLF and right PC contributed significantly to the association with *d′*.

Planned follow-up analyses were contingent on observing significant results in the primary analyses. All models described below included age as a covariate.

First, contingent on the significant association with right PC, we investigated the relative contributions of right inferior and superior PC. Higher FA in right superior PC ($\beta = 0.287$, $t_{(73)} = 3.092$, $P = 0.0028$; Age: $\beta = 0.504$, $t_{(73)} = 5.427$, $P < 0.0001$; $R^2 = 0.405$) but not right inferior PC FA ($\beta = 0.142$, $t_{(73)} = 1.475$, $P = 0.15$; Age: $\beta = 0.556$, $t_{(73)} = 5.67$, $P < 0.0001$; $R^2 = 0.346$) was significantly associated with *d′*. This was even more evident when right superior and right inferior PC FA were entered simultaneously into one model ($R^2 = 0.406$; Age: $\beta = 0.500$, $t_{(72)} = 5.329$, $P < 0.0001$; right superior PC: $\beta = 0.271$, $t_{(72)} = 2.695$, $P = 0.0087$; right inferior PC: $\beta = 0.042$, $t_{(72)} = 0.419$, $P = 0.68$).

Next, to examine the anatomical specificity of observed associations between *d′* and right SLF and right superior PC FA, we included either global WM FA (mean TBSS skeleton FA), or FA of the corresponding left hemisphere ROI as additional predictors. The results of these regression models are presented in Tables IV and V for right SLF FA and right superior PC FA, respectively. Age was significantly associated with *d′* in all models. A graphical presentation of the significant positive association between right SLF FA and *d′* after adjusting for age (Table IV, Model 1) is depicted in Figure 5a. The association remained significant when global WM FA was entered as an additional covariate in the model (Table IV, Model 2), suggesting that the association was anatomically specific and not driven by general brain maturational increases in WM FA. The association between right SLF FA and *d′* also remained significant when left SLF FA instead of global WM FA was entered as an additional covariate, suggesting that the observed association was specific for the right hemisphere (Table IV, Model 3). While higher left SLF FA by itself was significantly and positively associated with *d′* (Table IV, Model 4, and Fig. 5b), this association became trend level when global WM FA was included in the model (Table IV, Model 5).

A graphical presentation of the significant positive association between right superior PC FA and *d′* after adjusting for age (Table V, Model 1) is depicted in Figure 5c. The association remained significant when global WM FA was entered as an additional covariate in the model (Table V, Model 2), suggesting that global increases in WM FA did not drive the relationship. Moreover, when including right and left superior PC in the same model, the right ROI continued to display significant associations with *d′* (Table V, Model 3), suggesting that the observed association between right superior PC and *d′* is anatomically specific. The left superior PC was by itself not significantly related to *d′* (Table V, Model 4).

To further explore the nature of the observed right SLF and superior PC FA effects, we examined $\lambda_\perp$ and $\lambda_\parallel$. Our analyses revealed that higher *d′* (better sustained attention performance) was significantly associated with lower $\lambda_\perp$ of both the right SLF ($\beta = -0.214$, $t_{(73)} = -2.077$, $P = 0.041$;

TABLE V. Follow-up analyses testing the specificity of right superior PC FA associations with RVP *d′*

				Age			Right superior PC FA			Left superior PC FA			Global WM FA		
Model	Dependent variable	R^2	*df*	β	*t*	*p*	β	*t*	*p*	β	*t*	*p*	β	*t*	*p*
1	*d′*	0.405	73	0.504	5.427	*0.0000007*	0.287	3.092	***0.003***						
2	*d′*	0.405	72	0.503	4.948	*0.0000048*	0.286	2.837	***0.006***				0.005	0.042	0.967
3	*d′*	0.409	72	0.510	5.452	*0.0000007*	0.305	3.166	***0.002***	−0.069	−0.730	0.468			
4	*d′*	0.327	73	0.570	5.877	*0.0000001*				0.008	0.085	0.932			

Multiple regression on the rapid visual information processing (RVP) measure d′ with age, and fractional anisotropy (FA) of white matter underlying right and left superior parietal cortex (PC), and global white matter (WM). Significant associations are printed italic, with those related to FA-measures additionally printed in bold.

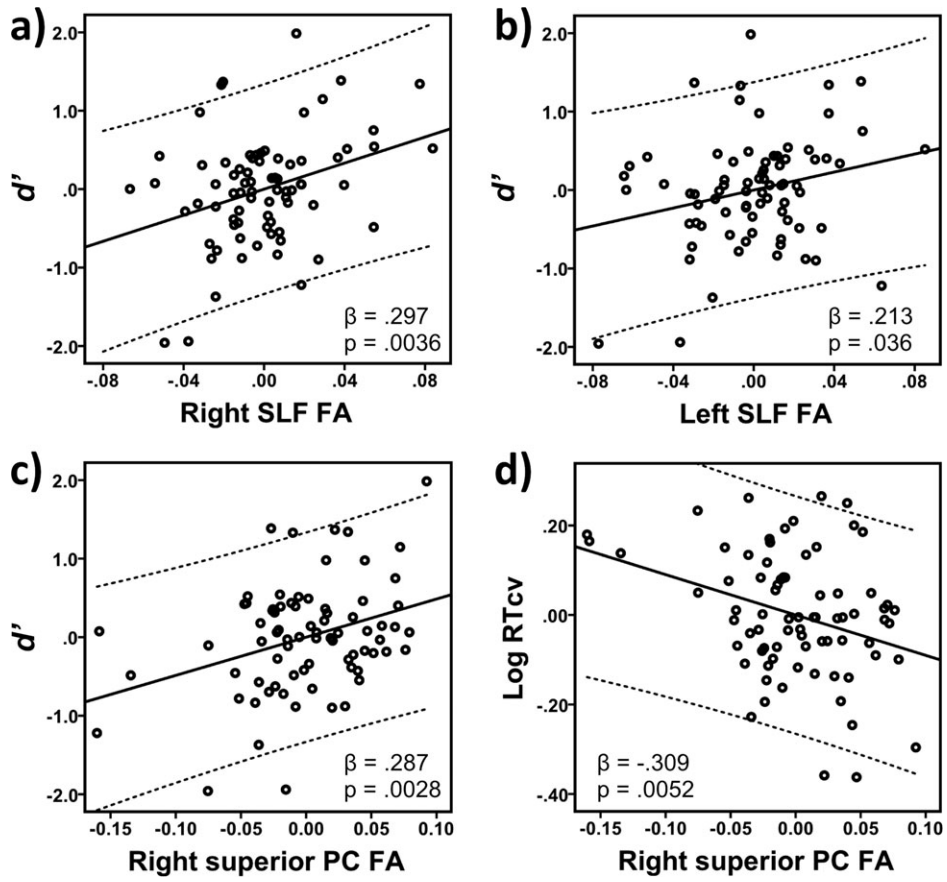

Figure 5.

Partial regression plots of the sensitivity measure d' as a function of fractional anisotropy (FA) within the (**a**) right superior longitudinal fasciculus (SFL), (**b**) left SLF, or (**c**) the white matter underlying the right superior parietal cortex (PC), adjusted for age. Independently of age, higher right and left SLF FA, and right superior PC FA were associated with better sustained attention performance as reflected in higher d' scores. While left SLF, when modeled separately, was significantly associated with d', after correcting for age, this association became non-significant when modeled together with the right SLF. (**d**) Partial regression plot of the logarithmically transformed coefficient of variation in reaction time (RT_{CV}) as a function of right superior PC FA, adjusted for age. Independently of age effects higher right superior PC FA was significantly associated with better sustained attention performance as reflected in lower RT_{CV} scores. The regression coefficient (β) and the significance level (P) for each FA variable are given in the lower right or left corner of each plot. Note that residuals are plotted after the effect of age was adjusted for.

Age: $\beta = 0.481$, $t_{(73)} = 4.669$, $P < 0.0001$; $R^2 = 0.364$) and right superior PC ($\beta = -0.269$, $t_{(73)} = -2.800$, $P = 0.007$; Age: $\beta = 0.489$, $t_{(73)} = 5.099$, $P < 0.0001$; $R^2 = 0.392$). Further, higher d' was significantly associated with higher right superior PC $\lambda_{\|}$ ($\beta = 0.209$, $t_{(73)} = 2.249$, $P = 0.028$; Age: $\beta = 0.587$, $t_{(73)} = 6.301$, $P < 0.0001$; $R^2 = 0.353$), but not with right SLF $\lambda_{\|}$ ($\beta = 0.141$, $t_{(73)} = 1.480$, $P = 0.143$; Age: $\beta = 0.555$, $t_{(73)} = 5.822$, $P < 0.0001$; $R^2 = 0.328$).

Associations Between RT_{CV} and the Right Fronto-Parietal Network

In addition to being related to d', higher FA in right superior PC was significantly associated with lower RT_{CV} scores (i.e., less variation in RT over time and thus more consistent and better sustained attention performance) (Table VI, Model 1, and Fig. 5d). No significant association was observed for the right SLF FA ($\beta = 0.036$, $t_{(73)} = 0.301$, $P = 0.764$; Age: $\beta = -0.351$, $t_{(73)} = -2.926$, $P < 0.005$; $R^2 = 0.115$). The RT_{CV} – right superior PC association showed anatomical specificity, as the association remained significant when global WM FA was entered as an additional covariate (Table VI, Model 2). Moreover, the association remained significant after controlling for left superior PC FA (Table VI, Model 3). Left superior PC FA by itself was not significantly associated with RT_{CV} (Table VI, Model 4). Age was significantly and negatively related to RT_{CV} in all models.

TABLE VI. Follow-up analyses testing the specificity of right superior PC FA associations with RVP RT_{cv}

				Age			Right superior PC FA			Left superior PC FA			Global WM FA		
Model	Dependent variable	R^2	*df*	β	*t*	*p*	β	*t*	*p*	β	*t*	*p*	β	*t*	*p*
1	*d′*	0.204	73	−0.264	−2.460	*0.016*	−0.309	−2.879	***0.005***						
2	*d′*	0.210	72	−0.231	−1.977	*0.052*	−0.278	−2.398	***0.019***				−0.091	−0.721	0.473
3	*d′*	0.175	72	−0.259	−2.389	*0.020*	−0.291	−2.609	***0.011***	−0.069	−0.625	0.534			
4	*d′*	0.133	73	−0.316	−2.873	*0.005*				−0.142	−1.294	0.200			

Multiple regression on the rapid visual information processing (RVP) measure coefficient of variation in reaction times (RT_{CV}) with age, and fractional anisotropy (FA) of white matter underlying right and left superior parietal cortex (PC), and global white matter (WM). Significant associations are printed italic, with those related to FA-measures additionally printed in bold.

Because right superior PC FA was related to both d' and RT_{CV}, and the behavioral measures were significantly correlated with each other ($r_{(74)} = -0.47$, $P < 0.001$), we tested to which extent each behavioral measure contributed to the other's association with right superior PC FA. RT_{CV} was entered as an additional covariate in the model predicting d' with age and right superior PC FA. Similarly, d' was entered as an additional covariate in the model predicting RT_{CV}. Our findings suggest that the association between right superior PC FA and d' is independent of RT_{CV} ($R^2 = 0.452$; Age: $\beta = 0.440$, $t_{(72)} = 4.710$, $P < 0.0001$; right superior PC: $\beta = 0.212$, $t_{(72)} = 2.239$, $P = 0.028$; RT_{CV}: $\beta = -0.243$, $t_{(72)} = -2.484$, $P = 0.015$) and that the association between right superior PC FA and RT_{CV} is independent of d' ($R^2 = 0.267$, Age: $\beta = -0.100$, $t_{(72)} = -8.17$, $P = 0.417$; right superior PC: $\beta = -0.216$, $t_{(72)} = -1.956$, $P = 0.054$; d′: $\beta = -0.325$, $t_{(72)} = -2.484$, $P = 0.015$).

Investigation of $\lambda_{\parallel}$ and $\lambda_{\perp}$ showed that lower RT_{CV} was significantly associated with lower $\lambda_{\perp}$ ($\beta = 0.331$, $t_{(73)} = 3.034$, $P = 0.003$; Age: $\beta = -0.235$, $t_{(73)} = -2.154$, $P < 0.035$; $R^2 = 0.213$), but not with $\lambda_{\parallel}$ ($\beta = -0.165$, $t_{(73)} = -1.520$, $P = 0.133$; Age: $\beta = -0.349$, $t_{(73)} = -3.206$, $P < 0.002$; $R^2 = 0.141$) of the WM underlying the right superior PC after adjusting for age.

Adjustment for Gender

Including gender as an additional covariate in the models did not change any of the observed associations between the behavioral and the ROI diffusion measures.

Effect-Size Map

The primary goal of this study was to test specific anatomical hypotheses about the relationship between microstructure of the WM underlying and connecting the right fronto-parietal cortices and variability in sustained attention performance in children. Therefore neither a whole brain, voxel-wise analysis of the effects (appropriately adjusted for test-multiplicity), nor a restricted voxel-wise analysis with small volume correction was deemed appropriate for testing these a priori hypotheses. However, since the analyses we used produce estimates of the effect size at each voxel, we have provided visualization of the effect-size maps. The effect size map visualizes regions where FA values are positively and negatively associated with d' independently of age (Fig. 6). The observed positive associations with the right and left SLF are visible in slice 33, and with the right superior PC in slice 54. In addition, positive associations with the WM underlying the left and right hand areas in the motor cortex (slice 54), the thalamic region (slice 14), and the WM underlying the lateral orbital gyrus bilaterally were observed. Furthermore, there was a negative association between d' and WM underlying the right superior temporal gyrus. The TBSS skeleton comprised a total of 103,588 voxels, of which 4,653 voxels had a t value above 1.993 and 1.469 voxels had a t value below −1.993 (uncorrected $P < 0.05$), corresponding to 5.91% of the total number of voxels in the skeleton. This percentage was 29.9% for the right SLF, 20.9% for the left SLF, 26.4% in the right superior PC, and 4.3% in the right inferior PC.

DISCUSSION

The present study revealed associations between sustained attention performance and WM microstructure in a large group of typically developing children aged 7–13 years. As hypothesized, right SLF, DLPFC, and PC FA were collectively associated with sustained attention performance independently of age. Specifically, the association was driven by right SLF and superior parietal FA. Both FA measures [Lebel et al., 2008, 2011] and performance on tests of sustained attention [Betts et al., 2006; Lin et al., 1999] are known to improve as a function of age in the investigated age range. Therefore simple correlations among these variables provide little evidence for any direct relationship between the WM measures and behavioral differences. Our findings suggest that even among children of similar age, higher FA in right SLF and superior PC is associated with better sustained attention performance. The associations between sustained attention performance and microstructure in right SLF and right superior PC appeared to be relatively anatomically specific, as they were independent of global WM FA. This is important, as FA is known to increase concurrently in many fibre tracts during childhood and adolescence. However, our results suggest that the present structure-

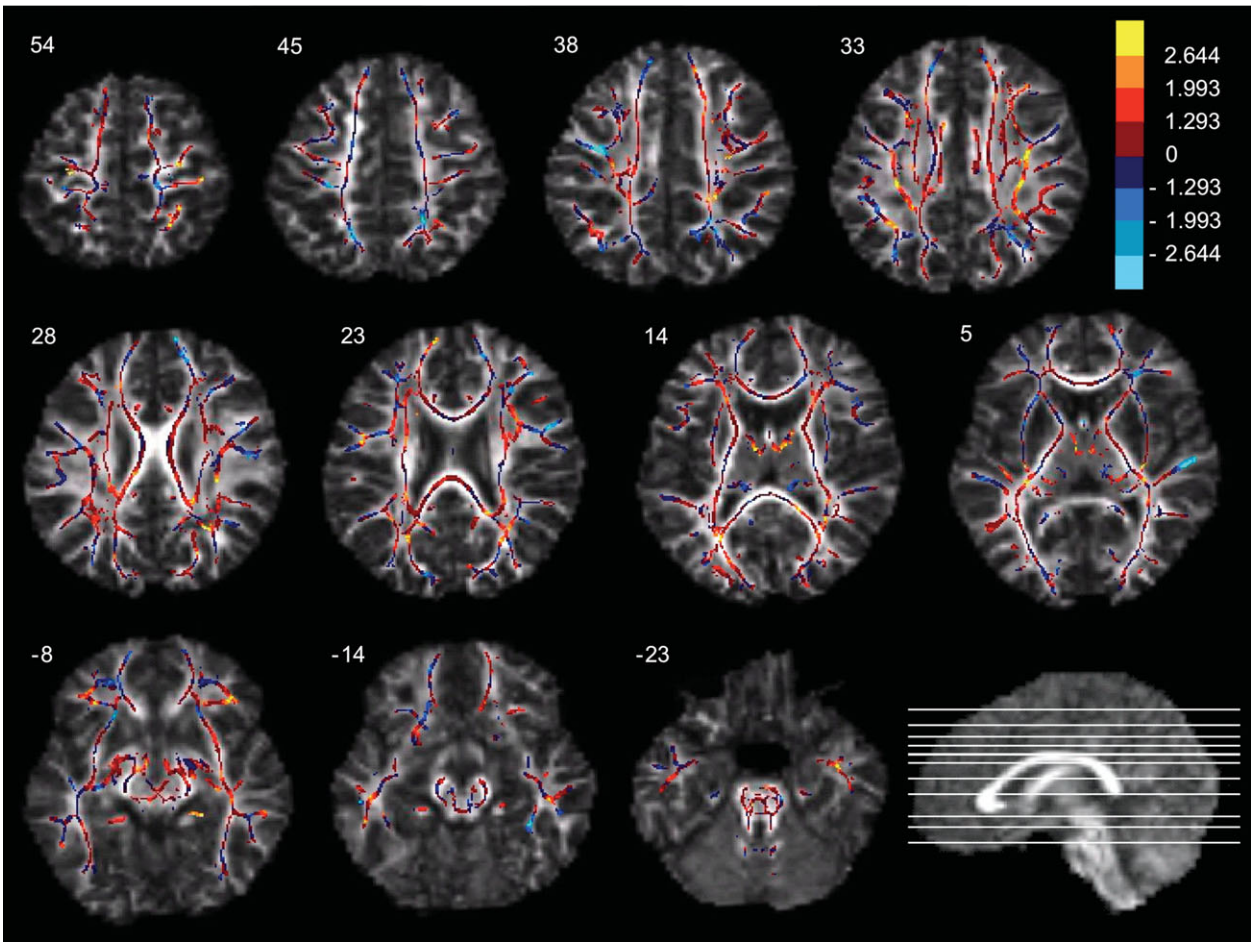

Figure 6.

Effect size map of the correlations between fractional anisotropy (FA) values and d' corrected for age. The voxels of the TBSS skeleton were color-coded according to the following voxel level t value cut-off points for both positive (red-yellow) and negative (blue-light blue) correlations ($df = 74$): $t = \pm 2.644$ ($P = 0.01$); $t = \pm 1.993$ ($P = 0.05$); $t = \pm 1.293$ ($P = 0.20$). Please note that these t values are not corrected for multiple comparisons. All images are axial slices presented with their MNI Z-coordinate. Left is left (neurological convention).

function relationships are unlikely to be mediated by a global increase in FA. Furthermore, the observed associations appeared to be relatively specific to the right hemisphere ROIs. The left superior PC was not associated with either d' or RT_{CV}, and the association observed between the left SLF and d' was, in contrast to the right side association, not independent of global FA. Also, when FA of both left and right SLF were modelled simultaneously, the left side association was no longer significant.

The analyses of $\lambda_{\perp}$ and $\lambda_{\parallel}$ showed that the associations between better sustained attention performance and higher ROI FA were primarily driven by decreased $\lambda_{\perp}$, and to a lesser extent increased $\lambda_{\parallel}$. Though the interpretation of changes in DTI parameters is not straightforward, previous studies suggest that $\lambda_{\perp}$ may be more sensitive to changes in myelination, extracellular volume fraction and axonal density [Beaulieu, 2009; Schwartz et al., 2005; Song et al., 2003, 2005]. Using a model of experimental de- and remyelination of the corpus callosum, a rodent study found that continuous cuprizone (neurotoxin) treatment caused demyelination of the callosal fibres, which was reflected by increased $\lambda_{\perp}$. The effects were reversed when the treatment was discontinued, and the progression of fibre remyelination was consistent with decreased $\lambda_{\perp}$ [Song et al., 2005]. Moreover, a study of the normal rat cervical spinal cord found that the perpendicular apparent diffusion coefficient (ADC) was positively correlated with extracellular volume fraction and axonal spacing, and negatively correlated with axonal number and myelination. Parallel ADC was found to be positively correlated with axonal diameter, and negatively with axonal number [Schwartz et al., 2005]. Although $\lambda_{\perp}$ does not measure

myelin, axonal diameter and density directly, these findings suggest that the degree of myelination, and axonal diameter and density to some extent may be contributing to the present findings. Further, age-related increases in FA have been linked to decreases in $\lambda_{\perp}$ [Lebel et al., 2008]. However, other factors, such as axonal tortuosity and organization, crossing fibres and tract geometry may also contribute to our findings in right SLF and superior PC FA [Beaulieu, 2009; Paus, 2010; Schwartz et al., 2005].

Our findings contrast somewhat with those of Mabbott et al. [2006], who did not observe any associations between FA of specific ROIs and sustained attention in children and adolescents after correcting for age. However, the ROIs applied in that study were 12 equal-sized large WM ROIs covering the whole brain, and 10 segmented fibre tracts not including the SLF, and thus the ROIs may have provided less sensitivity to the relevant fibre structures than did the present study. Furthermore, our finding of a right-lateralized network subserving sustained attention in children and adolescents differs from studies reporting a bilateral functional network for the RVP paradigm [Coull et al., 1996; Lawrence et al., 2003]. However, the RVP paradigms applied in these studies used either multiple target sequences or targets consisting of any three consecutive odd or even numbers. This substantially increased the working memory load of the tasks as compared to the RVP test used in the present study, where there was only one fixed target sequence. It might be that left hemisphere associations with RVP reflect demands on working memory rather than on sustained attention itself. This interpretation seems to be corroborated by the recent finding by our group, which showed that spatial working memory performance was specifically associated with FA of the left SLF in the same sample of subjects [Vestergaard et al., 2011]. These observations suggest an anatomical dissociation between sustained attention and working memory in the investigated age range, though it should be noted that it is unclear how spatial working memory demands might relate to the working memory demands of the different RVP tasks. Finally, other factors may contribute to the discrepancy between the right-sided findings in the present study and the more bilateral findings in other RVP-studies, e.g., differences in the age range of investigated subjects, or in the methods in general.

Contrary to expectations, we did not find an association between right DLPFC ROI FA and sustained attention performance. Reports of right DLPFC activations during simple sustained attention tasks [Coull et al., 1996; Lim et al., 2010; Pardo et al., 1991; Paus et al., 1997] suggested that such an association might be present. However, all of these studies were performed in adults. One of the possible explanations for not observing associations with right DLFPC FA in the age range investigated, might be regional differences in the phase of white matter maturation. Studies have suggested that frontal white matter may mature later than more posterior white matter [Colby et al., 2011; Lebel et al., 2008; Yakovlev and Lecours, 1967]. Thus, it may be that the white matter underlying the DLPFC matures later than the white matter in the PC and SLF ROIs. Alternatively, the DLPFC ROIs may be limited by low power or sensitivity, e.g., the DLPFC ROIs may include many other fibres than fibres from the SLF and thus these ROIs may have been a less sensitive index of the targeted fronto-parietal association fibres.

RT variability was measured using RT_{CV}, i.e., the SD of the RTs, divided by the mean RT. This approach was preferred to using the standard error of the mean of RTs, i.e., the SD divided by the square root of number of trials [Conners et al., 2003; Epstein et al., 2003; Hervey et al., 2006; Mabbott et al., 2006; Ogg et al., 2008; Yeo et al., 2003]. This latter measure may have an implicit accuracy bias in tests of sustained attention, since RTs are only produced for hits. Essentially, the standard error of the mean of RTs then becomes a RT variability score nonlinearly scaled by an accuracy score. This measure provides high diagnostic sensitivity and specificity [Epstein et al., 2003], but may be less suitable for localising neural substrates of cognitive processes because effects of accuracy and RT variability are conflated.

In the present study, d' was significantly associated with the WM microstructure of the right SLF and the right superior PC, while RT_{CV} only was associated with right superior PC. Furthermore, the association between right superior PC FA and d' was independent of RT_{CV}, and the association between right superior PC FA and RT_{CV} was independent of d'. The functional significance of these observed associations is unclear. Historically and theoretically sustained attention has been linked with accuracy measures (e.g., d'), while arousal has been associated with RT measures [Sturm and Willmes, 2001]. Although highly speculative, following the theory of sustained attention by Sarter et al. [2001, 2006], d' may be an expression of the "sustained attention network," including fronto-parietal connections such as SLF, while RT_{CV} might reflect the "arousal network," including thalamo-parietal connections. Further studies, employing tractography, functional MRI and TMS may be able to characterize these two putative networks.

Questions remain regarding the neurobiological interpretation of the age-independent relationships between sustained attention performance and diffusion parameters in the right SLF and superior PC. They may reflect individual differences in the phase of maturation of the right fronto-parietal system among children of similar age. This is likely, at least to some extent, since both sustained attention [Betts et al., 2006; Lin et al., 1999] and fronto-parietal WM microstructure [Lebel et al., 2008] continue to develop across the age range included in the present study. Alternatively, the variability in FA and $\lambda_{\perp}$ may reflect individual differences in the architecture of the right fronto-parietal system that emerge earlier in life during brain development, and remain stable in spite of superimposed biological changes associated with maturation. This is plausible since individual differences in

behavioral performance also have been associated with FA variability in adults [Gold et al., 2007; Wolbers et al., 2006]. Finally, the individual differences observed in the present study could also reflect variability in the experiences of the children. For example, Takeuchi et al. [2010] recently reported that the amount of time spent on training on a working memory task over a 2-month period was associated with increased FA in the WM underlying the intraparietal sulcus and in the anterior body of the corpus callosum. Longitudinal data analyses are a first step in disentangling the relative weight of stable characteristics, and maturational and/or experience driven dynamic processes.

CONCLUSION

Better sustained attention performance was found to be associated with higher FA and lower $\lambda_{\perp}$ in the right SLF as well as in the WM underlying the right superior PC. The associations displayed a higher level of specificity than found in earlier studies, as they were independent of age and global WM microstructure. The observed structure–function relationships could be due to stable individual differences, activity-dependent neuroplasticity, or to individual differences in the phase of maturation in the fronto-parietal network. Further studies including longitudinal data may provide further insights.

ACKNOWLEDGMENTS

The authors thank the children and their parents for their participation.

REFERENCES

Andersson JLR, Hutton C, Ashburner J, Turner R, Friston K. (2001): Modeling geometric deformations in EPI time series. Neuroimage 13:903–919.

Beaulieu C (2009): The biological basis of diffusion anisotropy. In: Johansen-Berg H, Behrens TE, editors. Diffusion MRI—From Quantitative Measurement to In-Vivo Neuroanatomy. London: Elsivier. p. 105–126.

Betts J, McKay J, Maruff P, Anderson V (2006): The development of sustained attention in children: The effect of age and task load. Child Neuropsychol 12:205–221.

Bonnelle V, Leech R, Kinnunen KM, Ham TE, Beckmann CF, De Boissezon X, Greenwood RJ, Sharp DJ (2011): Default mode network connectivity predicts sustained attention deficits after traumatic brain injury. J Neurosci 31:13442–13451.

Cabeza R, Nyberg L (2000): Imaging cognition II: An empirical review of 275 PET and fMRI studies. J Cogn Neurosci 12:1–47.

Cattapan-Ludewig K, Hilti CC, Ludewig S, Vollenweider FX, Feldon J (2005): Rapid visual information processing in schizophrenic patients: The impact of cognitive load and duration of stimulus presentation—A pilot study. Neuropsychobiology 52:130–134.

Chang LC, Jones DK, Pierpaoli C (2005): RESTORE: Robust estimation of tensors by outlier rejection. Magn Reson Med 53:1088–1095.

Cohen RM, Semple WE, Gross M, Holcomb HH, Dowling MS, Nordahl TE (1988): Functional localization of sustained attention: Comparison to sensory stimulation in the absence of instruction. Neuropsychiatry Neuropsychol Behav Neurol 1:3–20.

Colby JB, Van Horn JD, Sowell ER (2011): Quantitative in vivo evidence for broad regional gradients in the timing of white matter maturation during adolescence. Neuroimage 54:25–31.

Conners CK, editor (2000): Conners' Continuous Performance Test II: Computer Program for Windows Technical Guide and Software Manual. North Tonwanda, NY: Mutli-Health Systems.

Conners CK, Epstein JN, Angold A, Klaric J (2003): Continuous performance test performance in a normative epidemiological sample. J Abnorm Child Psychol 31:555–562.

Cook PA, Bai Y, Nedjati-Gilani SKKS, Hall MG, Parker GJ, Alexander DC (2006): Camino: Open-Source Diffusion-MRI Reconstruction and Processing. 14th Scientific Meeting of the International Society for Magnetic Resonance in Medicine, Seattle, WA, USA, p. 2759.

Corbetta M, Miezin FM, Dobmeyer S, Shulman GL, Petersen SE (1991): Selective and divided attention during visual discriminations of shape, color, and speed—Functional-anatomy by positron emission tomography. J Neurosci 11:2383–2402.

Cornblatt BA, Risch NJ, Faris G, Friedman D, Erlenmeyerkimling L (1988): The continuous performance-test, identical pairs version (Cpt-Ip) .1. New findings about sustained attention in normal-families. Psychiatry Res 26:223–238.

Coull JT (1998): Neural correlates of attention and arousal: Insights from electrophysiology, functional neuroimaging and psychopharmacology. Prog Neurobiol 55:343–361.

Coull JT, Frith CD, Frackowiak RSJ, Grasby PM (1996): A fronto-parietal network for rapid visual information processing: A PET study of sustained attention and working memory. Neuropsychologia 34:1085–1095.

Cowan N (1995): Attention and Memory: An Integrated Framework, Vol. 15. New York: Oxford University Press. pp 321.

Demeter E, Hernandez-Garcia L, Sarter M, Lustig C (2011): Challenges to attention: A continuous arterial spin labeling (ASL) study of the effects of distraction on sustained attention. Neuroimage 54:1518–1529.

Dineen RA, Vilisaar J, Hlinka J, Bradshaw CM, Morgan PS, Constantinescu CS, Auer DP (2009): Disconnection as a mechanism for cognitive dysfunction in multiple sclerosis. Brain 132 (Part 1):239–249.

Duvernoy HM, Bourgouin P (1999): The Human Brain: Surface, Three-Dimensional Sectional Anatomy With MRI, and Blood Supply. Wien, New York: Springer. pp 491.

Eluvathingal TJ, Hasan KM, Kramer L, Fletcher JM, Ewing-Cobbs L (2007): Quantitative diffusion tensor tractography of association and projection fibers in normally developing children and adolescents. Cereb Cortex 17:2760–2768.

Epstein JN, Conners CK, Sitarenios G, Erhardt D (1998): Continuous performance test results of adults with attention deficit hyperactivity disorder. Clin Neuropsychol 12:155–168.

Epstein JN, Erkanli A, Conners CK, Klaric J, Costello JE, Angold A (2003): Relations between continuous performance test performance measures and ADHD behaviors. J Abnorm Child Psychol 31:543–554.

Gold BT, Powell DK, Xuan L, Jiang Y, Hardy PA (2007): Speed of lexical decision correlates with diffusion anisotropy in left parietal and frontal white matter: Evidence from diffusion tensor imaging. Neuropsychologia 45:2439–2446.

Gong GL, He Y, Concha L, Lebel C, Gross DW, Evans AC, Beaulieu C (2009): Mapping anatomical connectivity patterns of human cerebral cortex using in vivo diffusion tensor imaging tractography. Cereb Cortex 19:524–536.

Hervey AS, Epstein JN, Curry JF, Tonev S, Arnold LE, Conners CK, Hinshaw SP, Swanson JM, Hechtman L (2006): Reaction time distribution analysis of neuropsychological performance in an ADHD sample. Child Neuropsychol 12:125–140.

Hilti CC, Delko T, Orosz AT, Thomann K, Ludewig S, Geyer MA, Vollenweider FX, Feldon J, Cattapan-Ludewig K (2010): Sustained attention and planning deficits but intact attentional set-shifting in neuroleptic-naive first-episode schizophrenia patients. Neuropsychobiology 61:79–86.

Jansons KM, Alexander DC (2003): Persistent angular structure: New insights from diffusion magnetic resonance imaging data. Inverse Problems 19:1031–1046.

Jernigan TL, Gamst AC, Fennema-Notestine C, Ostergaard AL (2003): More "mapping" in brain mapping: Statistical comparison of effects. Hum Brain Mapp 19:90–95.

Jovicich J, Czanner S, Greve D, Haley E, van der Kouwe A, Gollub R, Kennedy D, Schmitt F, Brown G, MacFall J, Fischl B, Dale A (2006): Reliability in multi-site structural MRI studies: Effects of gradient non-linearity correction on phantom and human data. Neuroimage 30:436–443.

Kim J, Whyte J, Wang J, Rao H, Tang KZ, Detre JA (2006): Continuous ASL perfusion fMRI investigation of higher cognition: Quantification of tonic CBF changes during sustained attention and working memory tasks. Neuroimage 31:376–385.

Klingberg T (2006): Development of a superior frontal-intraparietal network for visuo-spatial working memory. Neuropsychologia 44:2171–2177.

Konrad A, Dielentheis TF, El Masri D, Bayerl M, Fehr C, Gesierich T, Vucurevic G, Stoeter P, Winterer G (2010): Disturbed structural connectivity is related to inattention and impulsivity in adult attention deficit hyperactivity disorder. Eur J Neurosci 31:912–919.

Koski L, Petrides M (2001): Time-related changes in task performance after lesions restricted to the frontal cortex. Neuropsychologia 39:268–281.

Kurtz MM, Ragland JD, Bilker W, Gur RC, Gur RE (2001): Comparison of the continuous performance test with and without working memory demands in healthy controls and patients with schizophrenia. Schizophrenia Res 48:307–316.

Lawrence NS, Ross TJ, Hoffmann R, Garavan H, Stein EA (2003): Multiple neuronal networks mediate sustained attention. J Cogn Neurosci 15:1028–1038.

Lawrence NS, Ross TJ, Stein EA (2002): Cognitive mechanisms of nicotine on visual attention. Neuron 36:539–548.

Leark RA, Greenberg LK, Kindschi CL, Dupuy TR, Hughes SJ (2007): Test of Variables of Attention: Clinical Manual. Los Alamitos: The TOVA Company.

Lebel C, Gee M, Camicioli R, Wieler M, Martin W, Beaulieu C (2011): Diffusion tensor imaging of white matter tract evolution over the lifespan. Neuroimage 60:340–352.

Lebel C, Walker L, Leemans A, Phillips L, Beaulieu C (2008): Microstructural maturation of the human brain from childhood to adulthood. Neuroimage 40:1044–1055.

Lim J, Wu WC, Wang J, Detre JA, Dinges DF, Rao H (2010): Imaging brain fatigue from sustained mental workload: An ASL perfusion study of the time-on-task effect. Neuroimage 49:3426–3435.

Lin CCH, Hsiao CK, Chen WJ (1999): Development of sustained attention assessed using the continuous performance test among children 6–15 years of age. J Abnorm Child Psychol 27:403–412.

Mabbott DJ, Noseworthy M, Bouffet E, Laughlin S, Rockel C (2006): White matter growth as a mechanism of cognitive development in children. Neuroimage 33:936–946.

Madsen KS, Baaré WFC, Skimminge A, Vestergaard M, Siebner HR, Jernigan TL (2011): Brain microstructural correlates of visuospatial choice reaction time in children. Neuroimage 58:1090–1100.

Madsen KS, Baare WFC, Vestergaard M, Skimminge A, Ejersbo LR, Ramsoy TZ, Gerlach C, Akeson P, Paulson OB, Jernigan TL (2010): Response inhibition is associated with white matter microstructure in children. Neuropsychologia 48:854–862.

Molenberghs P, Gillebert CR, Schoofs H, Dupont P, Peeters R, Vandenberghe R (2009): Lesion neuroanatomy of the sustained attention to response task. Neuropsychologia 47:2866–2875.

Mori S, Wakana S, Van Zijl PCM (2004): MRI Atlas of Human White Matter. Amsterdam: Elsevier.

Ogg RJ, Zou P, Allen DN, Hutchins SB, Dutkiewicz RM, Mulhern RK (2008): Neural correlates of a clinical continuous performance test. Magn Reson Imaging 26:504–512.

Olesen PJ, Nagy Z, Westerberg H, Klingberg T (2003): Combined analysis of DTI and fMRI data reveals a joint maturation of white and grey matter in a fronto-parietal network. Cogn Brain Res 18:48–57.

Pardo JV, Fox PT, Raichle ME (1991): Localization of a human system for sustained attention by positron emission tomography. Nature 349:61–64.

Paus T (2010): Growth of white matter in the adolescent brain: Myelin or axon? Brain Cogn 72:26–35.

Paus T, Zatorre RJ, Hofle N, Caramanos Z, Gotman J, Petrides M, Evans AC (1997): Time-related changes in neural systems underlying attention and arousal during the performance of an auditory vigilance task. J Cogn Neurosci 9:392–408.

Perin B, Godefroy O, Fall S, de Marco G (2010): Alertness in young healthy subjects: An fMRI study of brain region interactivity enhanced by a warning signal. Brain Cogn 72:271–281.

Perrin JS, Leonard G, Perron M, Pike GB, Pitiot A, Richer L, Veillette S, Pausova Z, Paus T (2009): Sex differences in the growth of white matter during adolescence. Neuroimage 45:1055–1066.

Pfefferbaum A, Rosenbloom MJ, Fama R, Sassoon SA, Sullivan EV (2010): Transcallosal white matter degradation detected with quantitative fiber tracking in alcoholic men and women: Selective relations to dissociable functions. Alcohol Clin Exp Res 34:1201–1211.

Rao SM, Leo GJ, Bernardin L, Unverzagt F (1991): Cognitive dysfunction in multiple sclerosis. I. Frequency, patterns, and prediction. Neurology 41:685–691.

Reese TG, Heid O, Weisskoff RM, Wedeen VJ (2003): Reduction of eddy-current-induced distortion in diffusion MRI using a twice-refocused spin echo. Magn Reson Med 49:177–182.

Sarter M, Gehring WJ, Kozak R (2006): More attention must be paid: The neurobiology of attentional effort. Brain Res Rev 51:145–160.

Sarter M, Givens B, Bruno JP (2001): The cognitive neuroscience of sustained attention: Where top-down meets bottom-up. Brain Res Rev 35:146–160.

Scheperjans F, Eickhoff SB, Homke L, Mohlberg H, Hermann K, Amunts K, Zilles K (2008): Probabilistic maps, morphometry, and variability of cytoarchitectonic areas in the human superior parietal cortex. Cereb Cortex 18:2141–2157.

Schwartz ED, Cooper ET, Fan YL, Jawad AF, Chin CL, Nissanov J, Hackney DB (2005): MRI diffusion coefficients in spinal cord correlate with axon morphometry. Neuroreport 16:73–76.

Shallice T, Stuss DT, Alexander MP, Picton TW, Derkzen D (2008): The multiple dimensions of sustained attention. Cortex 44:794–805.

Smith SM, Jenkinson M, Johansen-Berg H, Rueckert D, Nichols TE, Mackay CE, Watkins KE, Ciccarelli O, Cader MZ, Matthews PM, Behrens TE (2006): Tract-based spatial statistics: Voxelwise analysis of multi-subject diffusion data. Neuroimage 31:1487–1505.

Snook L, Paulson LA, Roy D, Phillips L, Beaulieu C (2005): Diffusion tensor imaging of neuro development in children and young adults. Neuroimage 26:1164–1173.

Song SK, Sun SW, Ju WK, Lin SJ, Cross AH, Neufeld AH (2003): Diffusion tensor imaging detects and differentiates axon and myelin degeneration in mouse optic nerve after retinal ischemia. Neuroimage 20:1714–1722.

Song SK, Yoshino J, Le TQ, Lin SJ, Sun SW, Cross AH, Armstrong RC (2005): Demyelination increases radial diffusivity in corpus callosum of mouse brain. Neuroimage 26:132–140.

Stins JF, Tollenaar MS, Slaats-Willemse DIE, Buitelaar JK, Swaab-Barneveld H, Verhulst FC, Polderman TC, Boomsma DI (2005): Sustained attention and executive functioning performance in attention-deficit/hyperactivity disorder. Child Neuropsychol 11:285–294.

Sturm W, de Simone A, Krause BJ, Specht K, Hesselmann V, Radermacher I, Herzog H, Tellmann L, Muller-Gartner HW, Willmes K (1999): Functional anatomy of intrinsic alertness: Evidence for a fronto-parietal-thalamic-brainstem network in the right hemisphere. Neuropsychologia 37:797–805.

Sturm W, Willmes K (2001): On the functional neuroanatomy of intrinsic and phasic alertness. Neuroimage 14:S76–S84.

Sturm W, Willmes K, Orgass B, Hartje W (1997): Do specific attention deficits need specific training? Neuropsychol Rehabil 7:81–103.

Stuss DT, Murphy KJ, Binns MA, Alexander MP (2003): Staying on the job: The frontal lobes control individual performance variability. Brain 126:2363–2380.

Swets JA (1961): Is there a sensory threshold? Science 134:168–177.

Takahashi M, Iwamoto K, Fukatsu H, Naganawa S, Iidaka T, Ozaki N (2010): White matter microstructure of the cingulum and cerebellar peduncle is related to sustained attention and working memory: A diffusion tensor imaging study. Neurosci Lett 477:72–76.

Takeuchi H, Sekiguchi A, Taki Y, Yokoyama S, Yomogida Y, Komuro N, Yamanouchi T, Suzuki S, Kawashima R (2010): Training of working memory impacts structural connectivity. J Neurosci 30:3297–3303.

Vestergaard M, Madsen KS, Baaré WFC, Skimminge A, Ejersbo LR, Ramsøy TZ, Gerlach C, Åkeson P, Paulson OB, Jernigan TL (2011): White matter microstructure in superior longitudinal fasciculus associated with spatial working memory performance in children. J Cogn Neurosci 23:2135–2146.

Wechsler D (1981): Wechsler Adult Intelligence Scale—Revised. San Antonio, TX: The Psychological Corporation.

Wilkins AJ, Shallice T, Mccarthy R (1987): Frontal lesions and sustained attention. Neuropsychologia 25:359–365.

Wolbers T, Schoell ED, Buchel C (2006): The predictive value of white matter organization in posterior parietal cortex for spatial visualization ability. Neuroimage 32:1450–1455.

Yakovlev PI, Lecours AR (1967): The myelogenetic cycles of regional maturation of the brain. In: Minkowski A, editor. Regional Development of the Brain in Early Life. Philadelphia: F.A. Davis Co. p. 3–87.

Yeo RA, Hill DE, Campbell RA, Vigil J, Petropoulos H, Hart B, Zamora L, Brooks WM (2003): Proton magnetic resonance spectroscopy investigation of the right frontal lobe in children with attention-deficit/hyperactivity disorder. J Am Acad Child Adolesc Psychiatry 42:303–310.